The International Journal of Advanced Manufacturing Technology (2025) 137:2307–2317
https://doi.org/10.1007/s00170-025-15289-1

ORIGINAL ARTICLE

Sheet metal formability analysis by accessible and reliable digital image correlation system

Murilo do Nascimento Cruz[1] · Chetan P. Nikhare[2] · Ravilson Antonio Chemin Filho[1] · Paulo Victor Prestes Marcondes[1]

Received: 15 October 2024 / Accepted: 18 February 2025 / Published online: 27 February 2025

Abstract
The automotive industry is characterized by being a large consumer of stamped parts and by always looking for improvements in this process, aiming for more efficient products. This is since the vehicle body, basically made up of stamped parts, is highly representative of the total mass of the car, its safety, and drivability. Better results in stamping processes, however, can be achieved through better knowledge of the variables that affect the process, whose information base is still quite deficient in industries in general. Another important way to improve the processing of stamped parts is the development of more efficient materials, which have been evolving since the emergence of advanced high-strength steels (AHSS). Therefore, studies that make the effects of stamping tool parameters on the formability of metal sheets more understandable are of great relevance and are being carried out. However, more sophisticated techniques for monitoring the plastic deformation limit of sheets and the generation of more technological data are also essential. An existing technological resource for this is digital image correlation (DIC) systems, which are highly accurate and expensive. Thus, the present work aimed to develop a DIC system, initially implemented in a Nakazima stamping testing tool, to improve the analysis of the stampability of sheet metal, with possible application to tools in the industry. For this, high-resolution commercial cameras and open-source software were used, since, in addition to precision, the low cost of the system was also one of the objectives of the work. Thus, a sequence of stamping tests was carried out with BH220 steel, 1.5 mm thick, to capture images, which were later processed in software to graphically represent the deformations on the image of the stamped test piece. According to the results achieved, it was possible to attest to the efficiency of the developed DIC system, which proved to be very effective and practical for analyzing the deformations of metal sheets subjected to the Nakazima test.

Keywords Metal forming · Stamping · Nakazima test · Digital image correlation · Forming limit curve

1 Introduction

Despite the extensive knowledge of stamping procedures and other classic forming processes, the industrial scenario is still completely dependent on the personal experience of professionals who work in this area, which implies the need to implement more efficient techniques in these processes, aiming to improve the product quality, productivity, and cost reduction. Thus, one way to meet this need and generate technological data is to use more sophisticated techniques for monitoring the limit of plastic deformation of the metal sheet. Therefore, a technological resource that meets this need is digital image correlation (DIC) systems, which are very versatile and accurate, however, extremely expensive. Commercial solutions were mentioned by Jiang [1].

Based on this, an important research niche focuses on the development of an image acquisition system that is cheaper and no less efficient than existing systems, used by so many authors [2–9]. Opensource software allows for research and laboratory tests to evaluate the characteristics of the material in various areas like in-plane and out-of-plane measurement [10, 11], displacement/deformation and strain contours [12, 13], generating/registering test images [14, 15], and fatigue experimentation [16] which can also be implemented in industry tools. The use of high-resolution commercial cameras and open-source software was pointed out by Jiang [1]. Ncorr software, which was evaluated by Jorge et al. [17]

✉ Chetan P. Nikhare
cpn10@psu.edu

1 Mechanical Engineering Department, Federal University of Paraná, Curitiba, PR, Brazil

2 Mechanical Engineering Department, The Pennsylvania State University, Erie, PA, USA

and used by Kumar et al. [18] and Zheng et al. [19] in their works, is an option that allows for the creation of a low-cost DIC system, this being the main objective of this work.

Based on the proposed objective, the main stages of the work were to implement an image capture system for a Nakazima stamping test tool; also develop a DIC system for analyzing the formability of metal sheets in the Nakazima stamping test, using license-free software; and evaluate the assertiveness and points for improvement of the DIC system in evaluating the formability of steel sheets for the automotive industry.

1.1 Metal sheet forming evaluation

The Nakazima test is listed in ISO-12004–2 [20] as the test necessary to obtain a complete FLC (forming limit curve). The FLC is a classic tool for predicting the maximum formability of the material; a FLC is only valid for materials of the same class, thickness, and thermomechanical treatment. The FLC was developed by authors such as Keeler [21], Goodwin [22], and Woodthorpe et al. [23]; several authors used it as a tool in their work: Min et al. [24] evaluated the appearance of fractures due to the change in curvature on the surface of a metal sheet. Noder and Butcher [25] used the method of Min et al. [24] for a comparison in investigating the influence of this method for Nakazima and Marciniak tests. These tests were studied by Butcher et al. [26] to demonstrate that the use of Nakazima FLC data can lead to a physically inconsistent Marciniak model. Like Wang et al. [27], Butcher et al. [26] used a DIC system to form strains measurement.

The present study has conducted a comprehensive experimental characterization of a DP1180 advanced high-strength steel with relatively low formability to demonstrate that the use of Nakazima FLC data can lead to a physically inconsistent MK model.

Due to the wide use of different materials and expansion in the formability study of manufacturing processes, evaluation assets are essential to obtain more assertive methodologies and improve the technology involved in the process. Górszczyk et al. [28] presented the advantages and limitations of DIC (digital image correlation). The authors point out how the technology involved in the process enables deformation analysis for various engineering scenarios for a wide range of materials (Fig. 1, Surajit [29]).

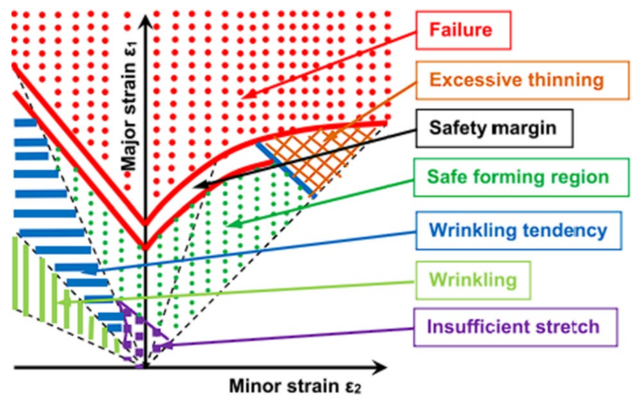

Fig. 1 Schematic representation of the FLD showing the safety limits for forming, Surajit [29]

DIC is an optical method that uses image tracking and registration techniques for precise 2D and 3D measurements of changes in images. This method is often used to measure total field displacements and strain and is widely applied in many areas of science and engineering. Compared to strain gauges, the amount of information collected about the fine details of strain during mechanical testing is increased due to the ability to provide local and average data using digital image correlation.

The analysis first consists of having a standard established so that the software and alike can record the initial and final images from these references (Górszczyk et al. [28]). This way, it is possible to verify differences in the images and these can be interpreted as deformations in the materials. The authors also explore the use of DIC in various scenarios using conventional equipment, such as traditional cameras (Górszczyk et al. [28]) and accessible Open-Source software (Belloni et al. [30]).

Kwiecién et al. [31] demonstrated the possibility to use DIC methodology to analyze deformations, and how it can be implemented in tests that analyze deformations and the onset of necking (Fig. 2, Kwiecién et al. [31]). This work by Kwiecién et al. [31] also compares simulation methods to whether DIC analysis matches expectations.

Leonard et al. [32] explained in their work how image correlation analysis influenced the improvement of the time-dependent method. This method consists of analyzing, through DIC, the beginning of deformations and consequently the beginning of necking in the metal sheet fracture. The following graphic (Fig. 16, Leonard et al. [32]) demonstrates from a deformation over time perspective, how it is possible to notice the moment when a more abrupt deformation than normal begins. Consequently, it is possible to correlate through DIC, which collects the deformation data at various moments and determines the beginning of the necking.

In the work of Martinez-Donaire et al. [33], work and other authors (Leonard et al. [32] for example) discussed that the best way to correlate time, space, and deformation data in these traditional tests for determining conformation limits is through DIC analysis.

With periodic image capture, it is possible to monitor the sample at different stages and consequently observe its deformations. Figure 3 exemplifies how it is possible, by monitoring the same sample section during a strain test, to observe the point of greatest strain in the sample and its

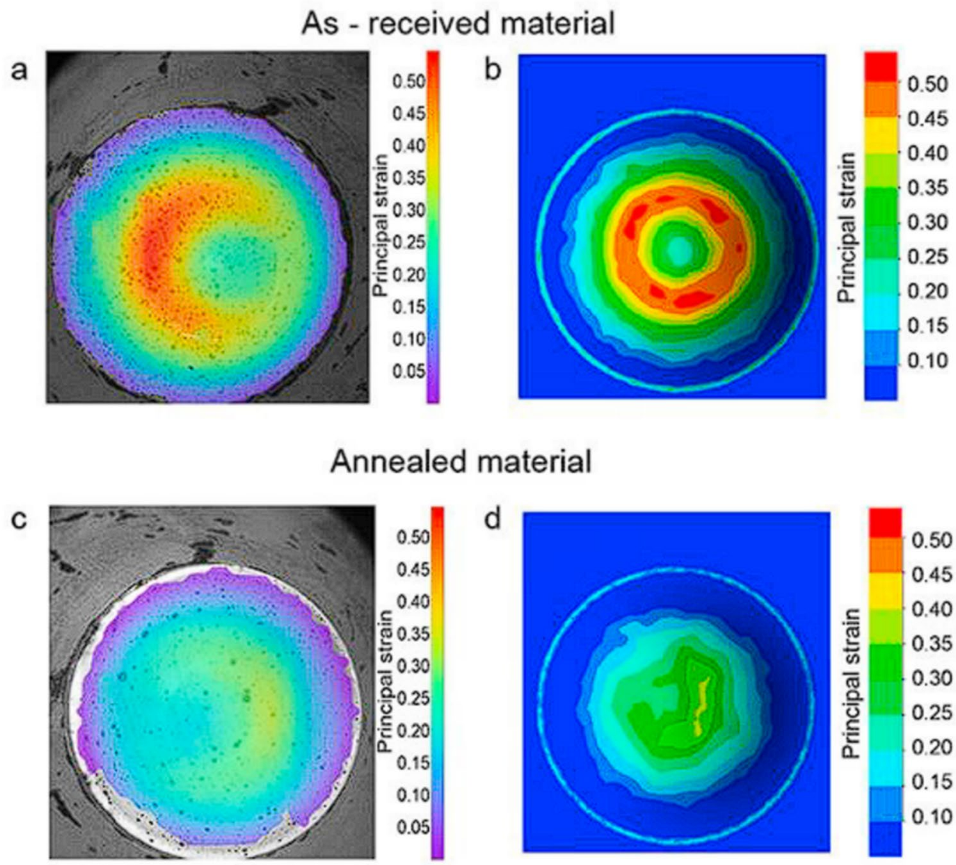

Fig. 2 Comparison of DIC analysis with CAE simulation for the same material received from the supplier and after annealing, Kwiecién et al. [31]

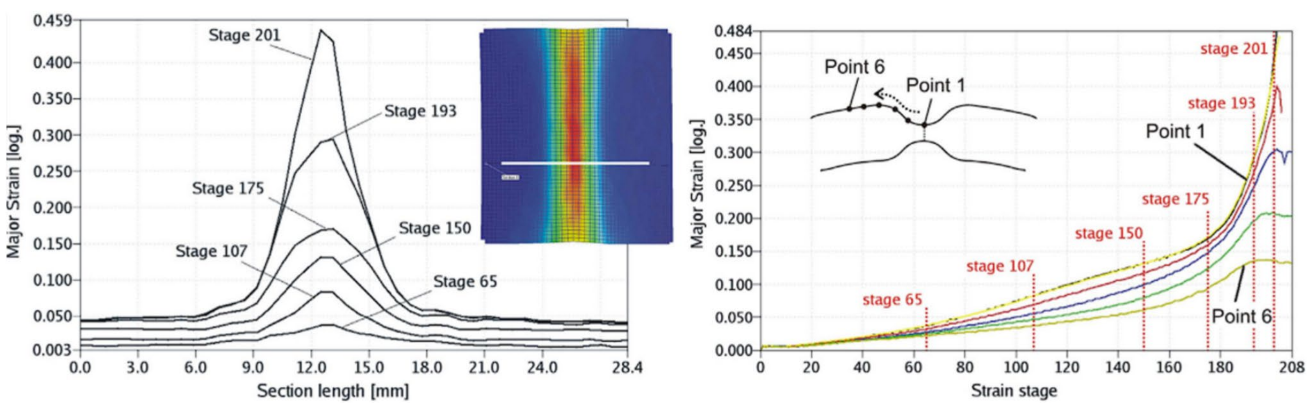

Fig. 3 DIC analysis of the sample section to find a point of greatest deformation and evolution of the necking region through image recording stages, Martinez-Donaire et al. [33]

evolution through stages, in the case of DIC analysis, corresponding to the frames during image recording.

Martinez-Donaire et al. [33] reinforced that the temporal method analysis consists of determining the starting point diffusion of the necking with the greatest strain, which would correspond to the center of the necking region. At this central point, the largest strain ε1 at the start of necking that will be used in this new FLC is formed from the temporal method. Figure 4 illustrates that the point determined as the start of necking is determined by the highest value of the strain rate at point A.

For Martinez-Donaire et al. [33], this point is the starting point of the necking region. ε1 is the central point value of the necking region when the strain rate at point A is maximum. The search for the necking point to perform DIC analysis is still widely explored in recent works such as Mu et al.

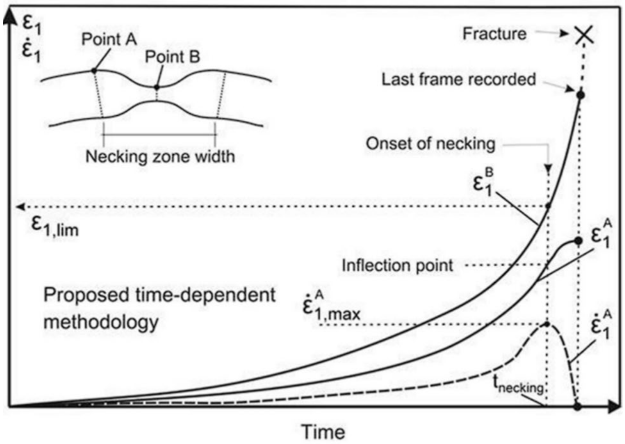

Fig. 4 Evolution of deformation and deformation speed at points A (outside the necking region) and B (localized necking point) to determine the start of necking from the drop in deformation speed at point A, Martinez-Donaire et al. [33]

[34] who performed a similar analysis focused on uniaxial stress through an anisotropic model.

Finally, the authors generated the FLC again through this correction of the temporal method to justify that it is a more assertive and real method when analyzing conformation limits, since in real scenarios, it is desirable to maintain the characteristics of the material before the necking point after the deformation.

Zhang et al. [35, 36] highlighted the possibility to use the temporal method to validate a process to determine the formability of the material. In previous works, these authors had already developed new forms of tools or samples to serve as a method analogous to traditional methods, such as Nakazima and Marciniak. In this specific validation topic, Zhang et al. [35, 36] used CAE simulations and numerical comparisons to determine whether the model proposed by them is in fact consistent with the traditional ones. The numerical calculation involved ended up comparing radial deformation by thickness, which is a form of analysis using the temporal method. And finally, they used DIC images (Fig. 5) to see if the necking starting point of the proposed model matched that analyzed in DIC in the traditional Nakazima test.

This session demonstrates how analysis using DIC has been widely used recently by several authors [6, 8, 9, 37] and how the results are increasingly assertive and with fewer empirical needs. The temporal method also ends up being a method to be explored in the other FLC works explored in this session and with great potential. Using

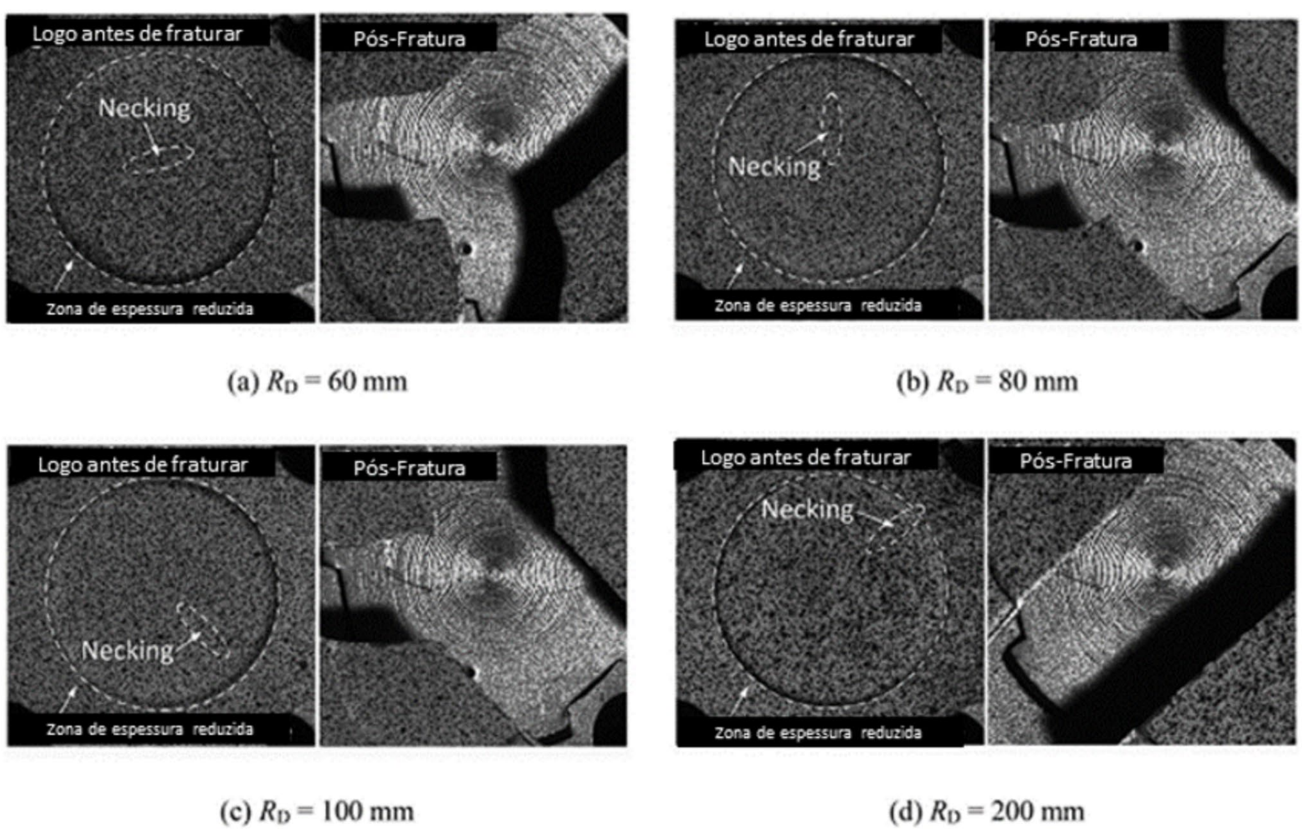

Fig. 5 Metallographic analysis to detect necking of specimens just before fracturing and post-fracture, Zhang et al. [35, 36]

this information with more recent methodologies and applying it to the tooling variables already known from those discussed previously to verify the influence is interesting for this study.

2 Methodology

The material used in the work was a BH220 steel sheet with 1.50 mm thick. Mechanical properties of this steel are given in Table 1. The objective of this study was to make the DIC system functional for use in stamping tests.

Table 1 Properties of BH220 steel (Information provided by ArcelorMittal steel supplier)

BH220 properties	
Yield strength (MPa)	210–270
Ultimate tensile strength (MPa)	320–400
Elongation (%) 50 mm	34
Elongation (%) 80 mm	32
Strain hardening	0.16

Elongation (%) 50 and 80 mm, percentage of elongation of a sample until fracture L_0 of 50 and 80 mm, ISO 6892–1 type 2 (EN20X80) and ISO 6892–1 type 1 (ASTM 12.5X50), respectively

For the biaxial stamping tests carried out with BH200 steel, the tooling used was similar as shown in Fig. 6 (Oliveira et al.; 2022) [38]. It can be seen from Fig. 6 that it is a tool with a hemispherical punch, with a diameter of 100 mm, following the Nakazima test standard. The tool also features an insert for assembling different interchangeable drawbeads, allowing for the tests, and the possibility of choosing four rings with different geometries (Fig. 6).

According to the drawbead geometries presented in Fig. 6, two options were selected for this work: A, with a flat drawbead (flat surface, without the bead), and B, with a circular profile drawbead, with a radius of 4 mm and height of 3 mm.

To capture the test images, a portable sport camera was attached to the tool. The camera is a small attachable sport camera with a 170° angular lens; video footage was recorded at 1080 p resolution at 30 frames per second. The camera was positioned inside the die and pointed in a direction perpendicular to the specimen during forming. In addition to the camera, an internal lighting system and special lenses were used for adequate framing and focusing of the generated images. Video footage is transmitted from the camera to a proprietary app via Wi-fi communication (Atrio Fullsport Cam). All tests were carried out in the forming laboratory at the Federal University of Paraná. No lubrication was used in the tests.

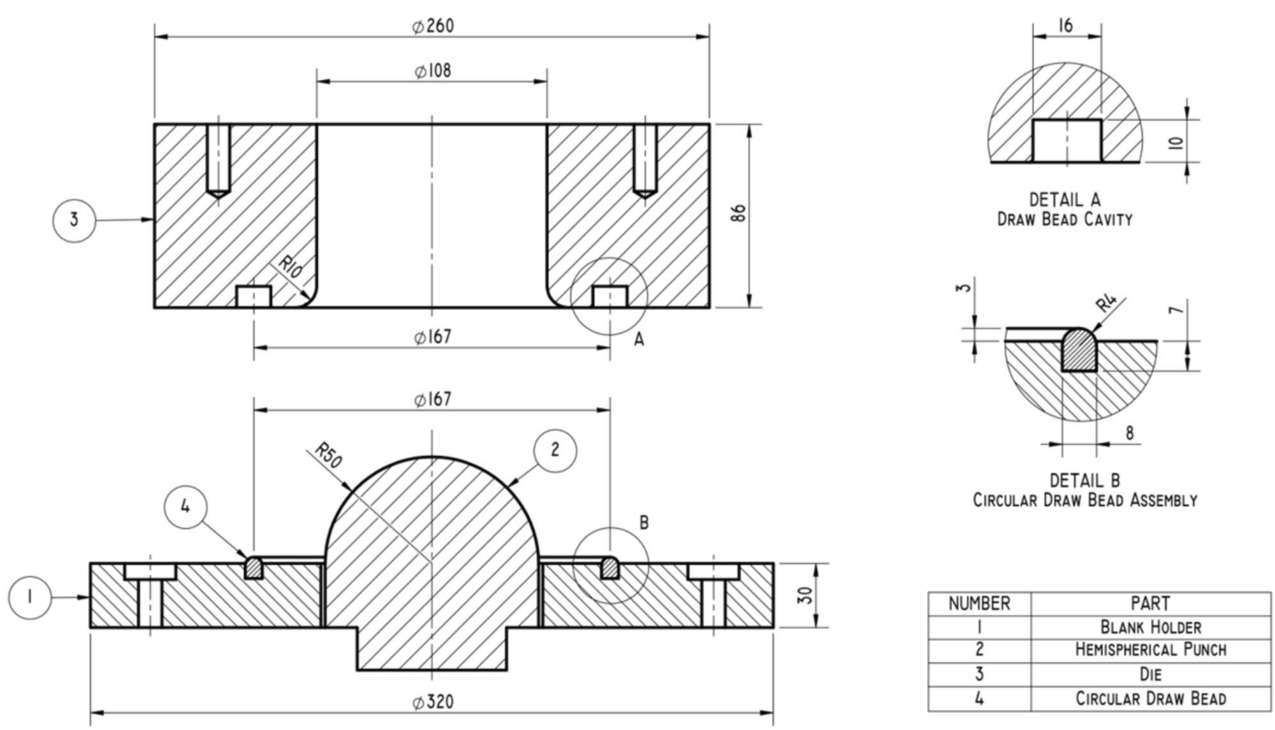

NUMBER	PART
1	BLANK HOLDER
2	HEMISPHERICAL PUNCH
3	DIE
4	CIRCULAR DRAW BEAD

Fig. 6 Technical drawing of hydraulic press equipment with a hemispherical punch with a radius of 50 mm following the Nakazima test standard. Configuration with circular drawbead, Oliveira [38]

Test bodies with geometries measuring 200 mm in length and eight different width dimensions were defined for the development stage of the DIC system, carried out with BH220 steel. Figure 7 shows the dimensions of the specimens used in the Nakazima tests. All specimens were cut using a guillotine, and subsequently, a mesh of circles was printed, using a silkscreen process on their surface to measure deformations. In all cases, the length of the specimens is in the rolling direction.

Each test was repeated successively, until functionality and subsequent calibration of the DIC system were achieved. At this stage, in addition to the flat and circular drawbeads, two different blank holder forces were used: 569 KN and 785 KN.

3 DIC system development

3.1 Analysis through digital image correlation

To capture images during deep drawing Nakazima tests, it was necessary to use a high-resolution camera with a special system of added lenses, positioned inside the die, to obtain images perpendicular to the strain region on the sheets, at sufficient resolution levels for subsequent analysis. A single-camera setup was built rather than a multiple-camera setup as seen in other authors' works; a single-camera setup requires less resources and no necessity of image merging for software analysis. Many authors used specific software for DIC analysis, and there is currently open-source software that does not depend on a license or any other type of intermediary to be used for the results of this work [1].

The hydraulic press used for the work has a PLC recording and control for the test with punch advance data and force per period as pointed out in the work of Chemin et al. [39], Lima et al. [40], and Lima et al. [41]. The deformations of the samples that made up the deformation axis of the results came from the DIC analysis. By moving away from the original pattern that was marked on the sample, the software allowed the image to be analyzed gradually, and thus represent the degree of deformation of the sheet based on the distancing of this initial pattern.

In the case of material studies with DIC analysis, these differences are interpreted as strains, since there is no relative movement between the device that acquires the images (camera) of the material.

In the studies cited in the bibliographic reference and for this work, the images for analysis are taken from a video recording. Separating into frames for a comparison of each frame, what was selected for this work were excerpts of 5-s recordings divided into frames for each 0.1-s interval. It is important for the time variable to be well defined to analyze the results and plot the graphics.

DIC analysis consists of comparing pixels by coordinates and checking whether there has been a change in their depiction. Therefore, to assist in the ease of DIC analysis, images with a high level of contrast are preferable, thus enabling easy identification of differences between pixels. For this work, it was necessary to check and analyze the results obtained by the tested software, also considering the feasibility and reliability of the data when discussing the results. Finally, according to the information carried out by Jiang [1] and Jorge et al. [17], the Ncorr software was tested to analyze its feasibility of use for the work. The Ncorr software was also used as one of the validation criteria in the same work by Belloni et al. [30] as a reference for DIC software as it is more renowned and has a reasonable number of citations in other works. The software for this work ran

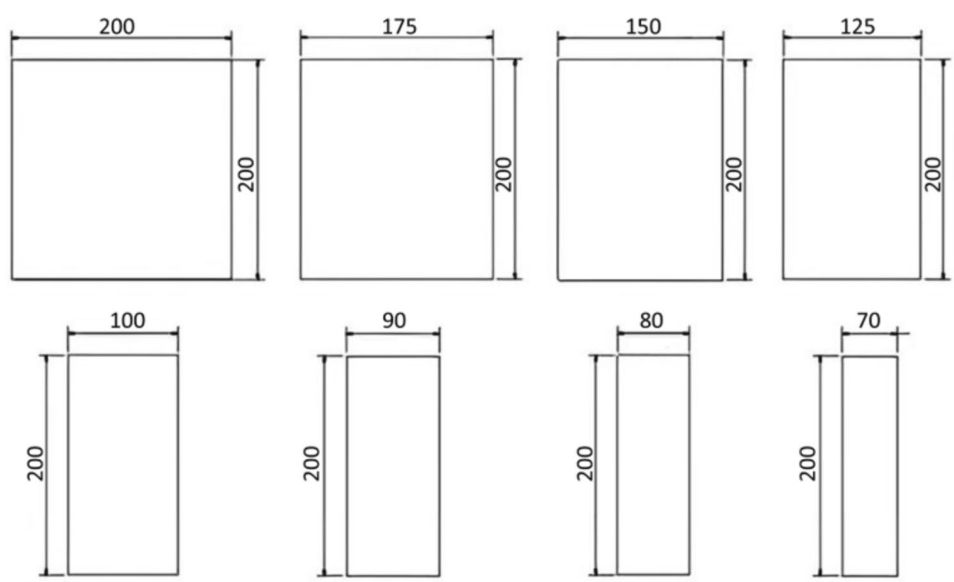

Fig. 7 Dimensions of test specimens used in tests for the development of the DIC system with BH220 steel. 8 samples from 200 × 200 to 70 × 200 mm, Oliveira [38]

on a mid-range computer with Matlab Software running on Windows Operational System.

For biaxial tests such as deep drawing, the use of two or more cameras is common, so that when joining images, it avoids any distortion arising from the distance to the stamped part; however, in the UFPR Forming Laboratory, image acquisition works better and is more feasible with the use from just one camera. Due to this, the tests with the DIC system developed were carried out just for bigger specimens with 200 mm width. Centeno et al. [4], Sharma et al. [8], and Abedine et al. [37] used two cameras in their works, to the Nakazima test (FLD), tension test section reduction, and incremental forming, respectively. The mirror-assisted multi-view system, presented by Chen et al. [42], is a possible equipment to replace a second camera on DIC analysis.

The small portable camera purchased to capture images can communicate via Wi-Fi. With the practical test recording, the section in which the rupture occurred was selected, and then, the moments before and after were cut, shortening the video.

An important factor to be considered when capturing the image is lighting, as inside the press chamber the image ends up being dark and unsuitable for analysis on the computer. To solve this problem, a light source was needed to adhere to the camera. The module consisted of a camera, a light source, a corrective lens, and a magnet for attachment. The corrective lens served to ensure the framing of the entire specimen in the image.

4 Results and discussion

For Ncorr software, all the necessary data for analysis are inserted, mainly the images, and the parameters offered by the software were established. The software also requires the insertion of a region of interest, which is determined by the user, and in this study, the entire region of the sample was selected. Once the analysis was completed, the displacements and deformations identified were observed. These data are presented illustratively for each pixel of the 2D image in X and Y coordinates for all frames (Fig. 8).

Figure 8 represents the main strain region according to the software is the region where the failure occurred, pointing for accuracy from the software. For each coordinate, Ncorr returns a displacement value in X and Y, determined from U and V, respectively. In addition, returning deformation values Exx, Exy, and Eyy, which are the Green-Lagrangian or Eulerian-Almansi deformations (Blaber and Antoniou, 2017) [43] are used in this work. These deformations will be converted to true deformations according to Eqs. (1) and (2), adapted from Yang et al. [44]:

$$\varepsilon_1 = \frac{1}{2}\ln\left(E_{xx} + 1\right) \tag{1}$$

$$\varepsilon_2 = \frac{1}{2}\ln\left(E_{yy} + 1\right) \tag{2}$$

With consideration of plane stress state without angular distortion, the data was used for comparison. For this case, if Exx is on the axis of greatest deformation, it may be the opposite depending on the positioning of the fracture; it is up to the analysis for each case.

In summary, Ncorr records a total of 5 values for each image coordinate for each frame. This data is recorded in a.mat file, in value data tables. This work performs the analyses of these data tables, migrating them to Excel (Table 2). The fracture starting point is the region of maximum deformation. Based on the evolution of the crack, the other points will be indicated through the strain rate at the beginning of the region of necking diffusion. These

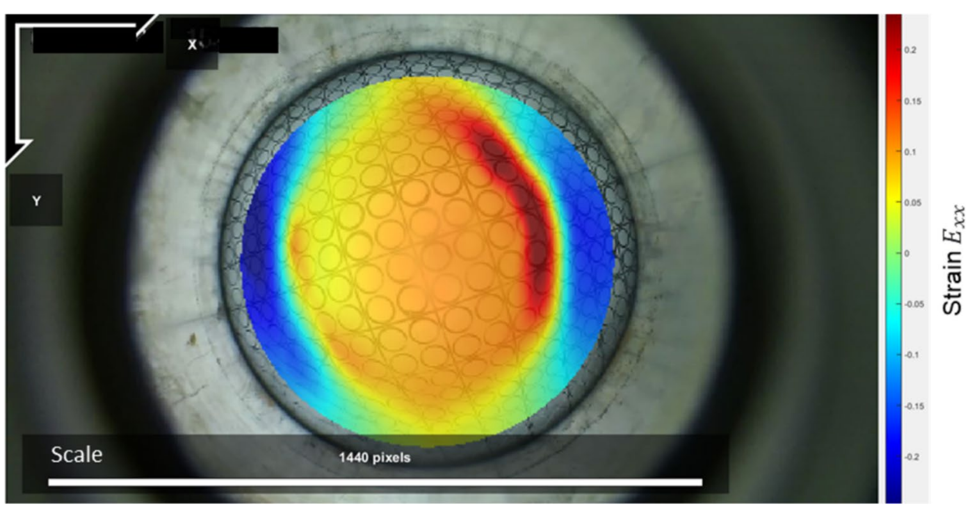

Fig. 8 Deformation map after image adjustment, with the area of maximum deformation in the fracture region

points are (A), (B), (C), (D), and (E), and all analyses are on the X and Y axes.

A DIC analysis reviews strains through the distance of pixels when compared to a reference image; looking through this perspective, Ncorr did not make a mistake as the center widened during the test. This can be easily demonstrated by comparing images Fig. 9a and b. Therefore, the conclusion is that the software performed a good analysis of the image, but the image was not good enough quality for this.

With these points from (A) to (E) having their respective coordinates converted by the software, it is possible to follow each point at each stage defined by the analysis. When plotting the evolution of the deformations of these points across frames, and consequently over time, we have Fig. 10.

To finally determine the test methodology, it was necessary to work on adjustments such as lens and framing of the acquired images as much as possible so that these divergences between the software analysis results and the real data were as small as possible. Damaging image factors were due to the limited physical space between the camera and the steel sheet to be formed.

Reviewing the results obtained by the software, this divergence was not considered a software analysis error in the strain region. For all the images obtained in the tests analyzed, the expansion of the central region during recording is noticeable (Fig. 9). This factor is due to the filming conditions.

Eliminating this factor and looking through the results obtained for these tests, it is appropriate to point out that Ncorr presented a satisfactory image of the results meeting the objectives of this work.

The strain evolution analysis demonstrates how the software interprets the fracture. Strain rate evolution pointed out by the arrows in Fig. 11 does represent the moment of the footage that the fracture begins. Therefore, to perform the necking analysis using the temporal method, it is necessary to analyze the strain rate of these same points, making it possible to identify the phases of diffuse necking and localized necking. Using points (A), (B), (C), (D), and (E), it was possible to verify the evolution of the fracture and then obtain the maximum strain rate over time (Fig. 11).

With the plot from Fig. 11, it is possible to identify the fracture region of the specimen as well as observe a

Table 2 Presentation of deformation data extracted from the DIC Ncorr software. For deformations in E_{xx} and E_{yy}

	Frame					
	39	40	41	42	43	44
Strain E_{xx}						
A	0.098630	0.103902	0.110196	0.116810	0.126368	0.137360
B	0.098349	0.103156	0.109546	0.116179	0.125358	0.136203
C	0.093653	0.097862	0.103474	0.108430	0.116218	0.126100
D	0.089633	0.092976	0.097372	0.100439	0.105465	0.112719
E	0.085384	0.088406	0.092466	0.094995	0.099089	0.100224
Strain E_{yy}						
A	0.0530136	0.0552981	0.0565255	0.0572924	0.0593582	0.0613515
B	0.0563730	0.0586973	0.0600895	0.0610575	0.0629896	0.0653106
C	0.0589450	0.0612517	0.0627232	0.0639397	0.0656162	0.0683490
D	0.0610866	0.0633815	0.0648788	0.0663247	0.0677121	0.0707069
E	0.0631710	0.0654918	0.0670344	0.0687539	0.0698619	0.0726708

Deformations Green-Lagrangian as E_{xx} and E_{yy} were extracted from the DIC Ncorr software for each point (A), (B), (C), (D), and (E) for each frame (frame taken from the video recorded in the test). Points that have coordinates in the software and were chosen in the rupture region. For the graphs shown in the work, these deformations are always converted to the true deformations by Eqs. (1) and (2)

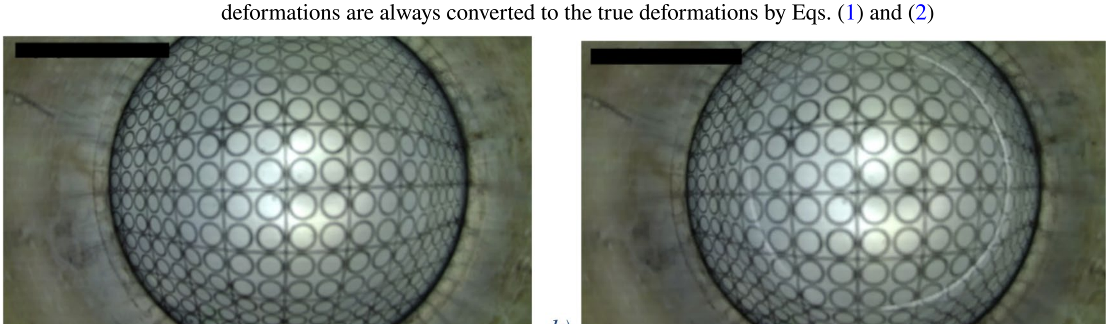

a) *b)*

Fig. 9 Images captured by the camera module inside the hydraulic press. **a** Test framework during stamping. **b** Test framework at the moment of rupture

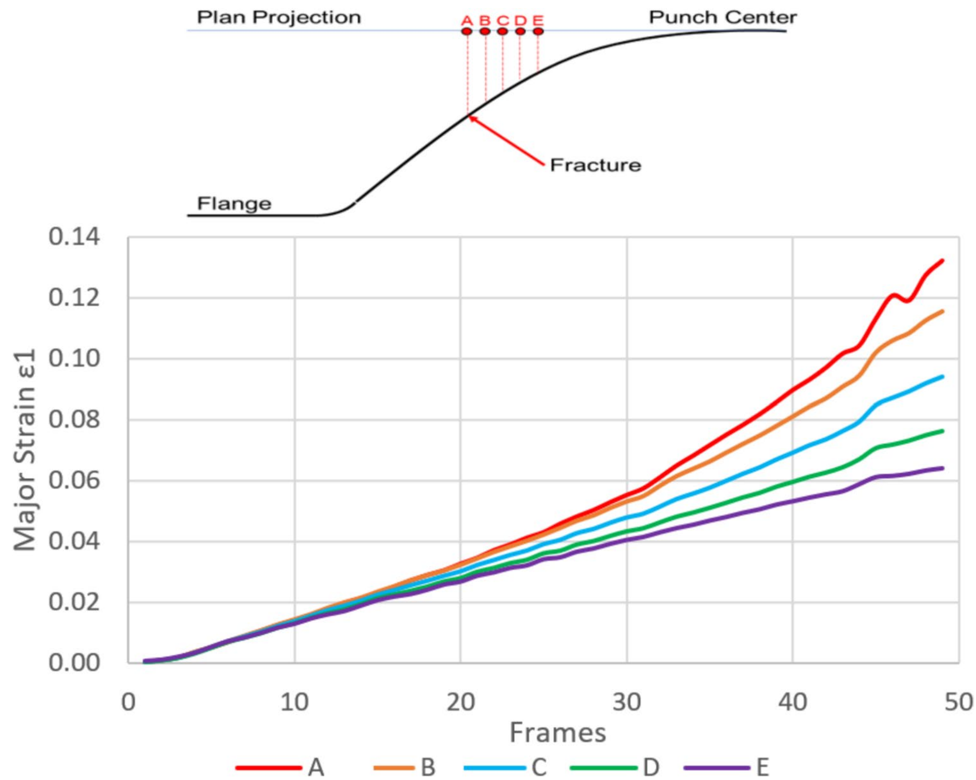

Fig. 10 Deformation evolution graph during forming in the fracture region after image adjustment during the development of the DIC software. Along the stamped profile of the sheet: (A) at the location of the fracture; (B), (C), (D) intermediate between the punch pole and the fracture; and (E) in the region of the punch pole, are points that are equidistant from each other

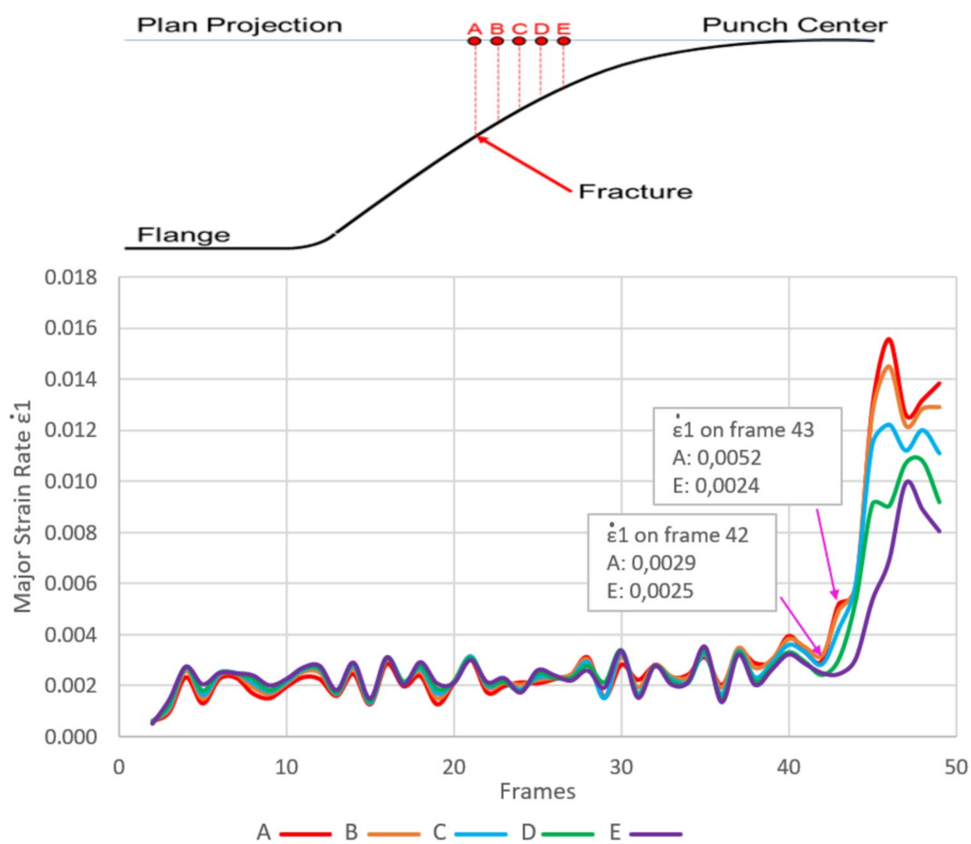

Fig. 11 Deformation rate graph during stamping in the fracture region after image adjustment during the development of the DIC software. This graph presents curves much closer to those expected in the literature, due to the image adjustment. Along the stamped profile of the sheet: (A) at the location of the fracture; (B), (C), (D) intermediate between the punch pole and the fracture; and (E) in the region of the punch pole, are points that are equidistant from each other

pre-rupture region that can be interpreted as the necking diffusion region. Materials that have greater elongation can better represent this region as they end up being more visible in the video and consequently better interpreted by the Ncorr software.

5 Conclusion

The methodology developed using DIC technology to increase the accuracy of forming results was achieved using laboratory systems and freely available software. The resulting plots allowed analysis of the deformation evolution of the tests along with the images collected in the tests.

After defining the reference image, the region of interest accommodated the entire sample, presenting a favorable deformation map for analysis. It was identified that in the end, the largest deformation spot on the deformation map was precisely in the fracture region and could be clearly identified.

As the punch rises, the sample approaches the camera, giving this depth effect, which for a purely two-dimensional analysis, as is understood for DIC analysis, is not desired. Various image capture equipment for DIC analysis uses more cameras or other devices that eliminate or mitigate this depth effect.

Strains deriving from greater angles concentrate in the center of the image, with less depth effect, which is desired for DIC analyses. Multiple-camera setup should be considered for future 3D measurement analysis and adjustment on DIC software accordingly.

Testing with this new module obtained different results in framing the sample image, ensuring that the fracture appeared completely within the video frame. Changes to image acquisition components ensured images with good focus and good image quality. The imaging results were more satisfactory.

The plot that showed the greatest evolution after image adjustment was that of the strain rate, with lines that were much more like the literature review. With the plot, it is possible to identify the fracture region of the specimen as well as observe a pre-rupture region that can be interpreted as the necking diffusion region.

Funding This research was funded by Gestamp Brasil Indústria de Autopeças S/A (sheet metal supply) and CNPq (Brazil).

Data availability Not applicable.

Code availability Not applicable.

Declarations

Ethics approval Not applicable.

Consent to participate Not applicable.

Consent for publication Not applicable.

Conflict of interest The authors declare no competing interests.

References

1. Jiang Z (2023) OpenCorr: an open-source library for research and development of digital image correlation. Opt Lasers Eng 165:107566
2. Agirre J, Galdos L, Argandoña ES, Mendiguren J (2018) Hardening prediction of diverse materials using the digital image correlation technique. Mech Mater 124:71–79
3. Aydin M, Wu X, Cetinkaya K, Yasar M, Kadi I (2018) Application of digital image correlation technique to Erichsen cupping test. Eng Sci Technol Int J 21:760–768
4. Centeno G, Martínez-Donaire AJ, Vallellano C, Martínez-Palmeth LH, Morales D, Suntaxi C, García-Lomas FJ (2013) Experimental study on the evaluation of necking and fracture strains in sheet metal forming processes. Proc Eng 63:650–658
5. Farahani BV, Belinha J, Amaral R, Tavares PJ, Moreira P (2018) A digital image correlation analysis on a sheet AA6061-T6 bifailure specimen to predict static failure. Eng Fail Anal 90:179–196
6. Jedidi MY, Valle V (2023) Experimental investigation to determine necking of commercially pure titanium sheets using a time-of-flight camera and Heaviside-digital image correlation. Opt Lasers Eng 164:107529
7. Pham QT, Islam MS, Sigvant M, Caro LP, Lee MG, Kim MS (2023) Improvement of modified maximum force criterion for forming limit diagram prediction of sheet metal. Int J Solids Struct 273:112264
8. Sharma M, Bhattacharya A, Paul SK (2024) Explicating tensile response of AA6061-T6 sheet post single point incremental forming: two camera-DIC strain measurement and texture analysis. Mech Mater 192:104963
9. Yu K, Li Q, Wu Y, Guo M, Li D, Liu C, Zhuang L, Wu P (2022) An improved Marciniak-Kuczynski approach for predicting sheet metal formability. Int J Mech Sci 221:107200
10. de Deus Filho JCA, da Silva Nunes LC, Xavier JMC (2022) iCorrVision-2D: an integrated python-based open-source Digital Image Correlation software for in-plane measurements (Part 1). SoftwareX 19:101131
11. Nunes L, Xavier J (2022) iCorrVision-3D: an integrated python-based open-source Digital Image Correlation Software for in-plane and out-of-plane measurements (Part 2). SoftwareX 19:101132
12. Das PP, Elenchezhian MRP, Vadlamudi V, Reifsnider K, André D, Raihan R (2024) RealPi2dDIC: a low-cost and open-source approach to In-situ 2D Digital Image Correlation (DIC) applications. SoftwareX 27:101864
13. Brisley, J. E. An open-source digital image correlation software system in Python (Doctoral dissertation, Stellenbosch University) (2024)
14. Rohe DP, Jones EMC (2022) Generation of synthetic digital image correlation images using the open-source blender software. Exp Tech 46(4):615–631
15. Chen B, Jungstedt E (2022) Fast and large-converge-radius inverse compositional Levenberg–Marquardt algorithm for digital image correlation: principle, validation, and open-source toolbox. Opt Lasers Eng 151:106930

16. Hebert J, Khonsari M (2023) The application of digital image correlation (DIC) in fatigue experimentation: a review. Fatigue Fract Eng Mater Struct 46(4):1256–1299
17. Jorge K, Ronny P, Sotomayor O (2022) On the digital image correlation technique. Mater Today Proc 49:79–84
18. Kumar SL, Aravind HB, Hossiney N (2019) Digital image correlation (DIC) for measuring strain in brick masonry specimen using Ncorr open source 2D MATLAB program. Results Eng 4:100061
19. Zheng Q, Mashiwa N, Furushima T (2020) Evaluation of large plastic deformation for metals by a non-contacting technique using digital image correlation with laser speckles. Mater Des 191:108626
20. ISO 12004–2. (2008) Metalic materials - Sheet and Strip - determination of forming-limit curve. [S.l.]: European Committee for Standardization, (2008).
21. Keeler SP (1965) Determination of forming limits in automotive stampings. Sheet Met Ind 42:683–691
22. Goodwin GM (1968) Application of strain analyses to sheet metal forming problems in the press shop. Metall Italiana 60:764–774
23. Woodthorpe J, Pearce R (1969) The effect of r and n upon the forming limit diagrams of sheet metal. Sheet Metal Industries 46:1061–1067
24. Min J, Stoughton TB, Carsley JE, Lin J (2016) Compensation for process-dependent effects in the determination of localized necking limits. Int J Mech Sci 117:115–134
25. Noder J, Butcher C (2019) A Comparative Investigation into the Influence of the Constitutive Model on the Prediction of In-Plane Formability for Nakazima and Marciniak Tests. Int J Mech Sci 163:105138
26. Butcher C, Khameneh F, Abedini A, Connolly D, Kurukuri S (2021) On the experimental characterization of sheet metal formability and the consistent calibration of the MK model for biaxial stretching in plane stress. J Mater Process Tech 287:116887
27. Wang K, Carsleyb JE, Hea B, Lic J, Zhang L (2014) Measuring forming limit strains with digital image correlation analysis. J Mater Process Technol 214:1120–1130
28. Górszczyk J, Malicki K, Zych T (2019) Application of digital image correlation (DIC) method for road material testing. Materials 12(15):2349
29. Surajit KP (2021) Controlling factors of forming limit curve: a review. Adv Ind Manuf Eng 2:100033
30. Belloni V, Ravanelli R, Nascetti A, Di Rita M, Mattei D, Crespi M (2019) PY2DIC: a new free and open-source software for displacement and strain measurements in the field of experimental mechanics. Sensors 19(18):3832
31. Kwiecién M, Lisiecki L, Lisiecka-Graca P, Majta J, Muszka K (2020) Study of deformation behavior of multilayered sheets using digital image correlation. Proc Manuf 47:1257–1263
32. Leonard, M. E., Signorelli, J. W., Stout, M. G., Roatta, A. Métodos Temporales para Determinar Deformaciones Límite en Chapas Metálicas. Revista Matéria (2018).
33. Martínez-Donaire AJ, García-Lomas FJ, Vallelano C (2014) New approaches to detect the onset of localised necking in sheets under through-thickness strain gradients. Mater Des 57:135–145
34. Mu Z, Zhao J, Gaochao Y, Huang X (2021) Hardening model of anisotropic sheet metal during the diffuse instability necking stage of uniaxial tension. Thin-Walled Structures 159:107198
35. Zhang R, Shi Z, Shao Z, Yardley VA, Lin J (2021) An effective method for determining necking and fracture strains of sheet metals. Methods 8:101234
36. Zhang R, Shi Z, Shao Z, Yardley VA (2021) Biaxial test method for determination of FLCs and FFLCs for sheet metals: validation against standard Nakajima method. Int J Mech Sci 209:106694
37. Abedini A, Narayanan A, Butcher C (2022) An investigation into the characterization of the hardening response of sheet metals using tensile and shear tests with surface strain measurement. Forces in Mechanics 7:100090
38. Oliveira AR, Lajarin SF, Rebeyca CJ, Chemin Filho RA, Nikhare CP, Marcondes PVP (2022) Influence of drawbead geometry and blank holder force on the dual phase steel formability. Int J Adv Manuf Technol 121:4255
39. Chemin Filho RA, Valente Tigrinho LM, Barreto Neto RC, Marcondes PVP (2013) An experimental approach for blankholder force determination for DP600 with different material flow strain rates in the flange during stamping. Proceedings of the Institution of Mechanical Engineers, Part B: Journal of Engineering Manufacture 227(3):417–422
40. Lima, E, Chemin Filho, R. A., Marcondes, P. V. P.. Avaliação do Limite de Estricção do Aço Dual Phase DP 600 Através da Curva Limite de Conformação. 37th SENAFOR, 7th International Sheet Metal Forming, (2017).
41. Lima E, Cruz MN, Chemin Filho RA, Nikhare CP, Marcondes PVP (2023) Influence of the hydraulic press system on advanced high-strength steel formability. Int J Adv Manuf Technol 126(2023):4722
42. Chen B, Pan B (2022) Mirror-assisted multi-view digital image correlation: principles, applications and implementations. Opt Lasers Eng 149:106786
43. Blaber, J., Antoniou, A. Ncorr instruction manual version 1.2.2. Georgia Institute of Technology (2017).
44. Yang, L., Smith, L., Gothekar, A., Chen, X. Measure strain distribution using digital image correlation (DIC) for tensile tests. The Advanced High Strength Steel Stamping Team of the Auto/Steel Partnership (A/SP) (2010).